High-Gain Thompson-Scattering X-Ray Free-Electron Laser by Time-Synchronic Laterally Tilted Optical Wave

Chao Chang, Chuanxiang Tang, and Juhao Wu

Phys. Rev. Lett. **110**, 064802 — Published 5 February 2013

DOI: 10.1103/PhysRevLett.110.064802

High-gain Thompson scattering X-ray Free Electron Laser by time-synchronic laterally tilted optical waves

Chao Chang,[1] Chuanxiang Tang,[2] and Juhao Wu*[1]

[1]*SLAC National Accelerator Laboratory, Stanford University, Stanford, CA 94309, USA*
[2]*Department of Engineering Physics, Tsinghua University, Beijing 100084, People's Republic of China*

A novel approach to generate coherent X-rays with $10^9 - 10^{10}$ photons and femtoseconds duration per laser pulse is proposed. This high intensity X-ray source is realized first by the pulse front tilt of lateral fed laser to extend the electron-laser synchronic interaction time by several orders, which accomplishes the high-gain Free-Electron-Laser-type exponential growth process and coherent emission with highly microbunched electron beam. Secondary, two methods are presented to enhance the effective optical undulator strength parameter. One is to invoke lenses to focus two counter-propagating lasers which are at normal incidence to the electron beam as a transverse standing wave; the other is to invent a periodic microstructure which can significantly enhance the center electromagnetic field realized by resonant standing wave and the quadrupole waveguides. The energy coupling efficiency between the electron beam and laser is therefore greatly improved to generate the high brightness X-rays, which is demonstrated by analytical and simulation results.

PACS numbers: 41.60.Cr, 42.25.Kb

Free-electron lasers (FEL) are the most powerful X-ray radiation sources to support many frontier researches; however, the large-scale magnetic undulator and RF electron accelerator limit only a few sources existed worldwide [1]. The optical undulator and laser-plasma accelerators on the other hand, may provide the potential to significantly reduce the size and cost of these X-ray sources to the university-laboratory scale [2–5].

For a nonlinear relativistic Thompson Scattering [6], the magnetic and electric fields of the light have the same effect on the electron motion, and electrons emit X-ray photons through the relativistic motion [7, 8]. The optical wave in the nonlinear Thompson Scattering serves as an electromagnetic undulator [9], whose periods are several orders-of-magnitude shorter than the conventional undulator with alternating static magnetic field used for synchrotron radiation or FEL. There are various applications of such Thompson/Compton X-ray sources including measurement of the plasma parameters in Z-pinch [10] and energy and energy spread of electron beam [11], imaging of atomic-scale spatial resolution [12], and biological and medical diagnostic systems.

The conventional method for Thompson Scattering using counter-propagating laser with electron beam has confronted bottleneck: the highest yield of X-ray flux was reported about 2×10^7 photons with several picoseconds duration [13]. The reason is that the interaction time for the close-to-speed-of-light electron beam and the counter-propagating laser mainly depends on the laser pulse duration. Thus, a long laser pulse is naturally demanded. For instance, in order to realize FEL in an optical undulator with a 10-20 gain length, *i.e.* about 3 cm long, an ultra-long 200 ps and ultra-intense Terawatt counter-propagating laser pulse is needed, which is hardly to realize. For a laser co-propagating with beam, the electric force and magnetic force on the relativistic electron cancel with each other, leading to a very low net field strength. Consequently, only incoherent or weak coherent radiation is emitted. In order to decrease the gain length and enhance the X-ray yield, increasing the beam current or decreasing the electron energy is proposed. For instance, electron beams with peak current 20 kA, low energy 30 MeV, emittance 0.3 πmm-mrad, and relative energy spread 0.4 % were proposed [14]; however, there is still no experimental demonstration on generating such an ultrahigh current and low energy beam. In Ref. [15], an electron beam of low energy 5.88 MeV, current 0.5 kA, and relative energy spread of 0.01 % is needed to interact with a Terawatt laser of 1 μm transverse spot size and 20 ps pulse duration to generate 0.3 MW X-ray. Consequently, how to realize 10^8 photons with femto-seconds duration in a single laser pulse is still a critical problem. In this letter, novel methods to significantly increase the coherent X-ray numbers by several orders with several femto-seconds duration are proposed, which may finally realize a table-top X-ray FEL envisioned by Ref. [16].

In our first method, after focused by cylindrical lenses, two counter-propagating laser pulses with the equal amplitude, same vertical electric polarization E_y and identical phase are at normal incidence to the electron-beam channel, as illustrated in Fig. 1. A standing wave along the optical propagation of x-direction is formed, which has a total y-polarized (pointing outward from the page) electric field with the expression of $2E_{y,m}(x,z)\cos(\omega t + \phi)\cos(kx)$, where ω, k, $E_{y,m}(x,z)$, ϕ are respectively the angular frequency, the wave number, the amplitude, and the injection phase of the laser; and the z-polarized magnetic field is parallel to the beam motion. The field amplitude of the standing wave at the central plane is strengthened because of the focus effect of the cylindrical lenses. Thus, at the central plane $x = 0$ of the beam channel, electrons undergo an intense transverse electric force

*Corresponding author: jhwu@SLAC.Stanford.EDU

$2eE_{y,m}(0,z)\cos(\omega t+\phi)$ and a negligible magnetic force. In this configuration, the undulator period is $\lambda_u = \lambda$, as compared to $\lambda_u = \lambda/2$ for a backward wave.

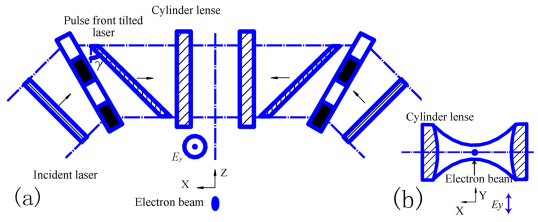

FIG. 1: Time-synchronic interaction of electrons with pulse front tilted lasers: (a) top view; (b) side view.

The time-synchronic interaction of the beam and waves is realized by the pulse front tilt, which is created by using an optical diffractive grating element with angular dispersion, as illustrated in Fig. 1(a), where γ is the tilt angle between the pulse front and the phase front. The pulses still have their phase front perpendicular to the propagation direction [17–19], but the arrival time of the laser pulse at interaction area is synchronously delayed with the electron beam flying. It is illustrated in Fig. 2 that electron beam moves along z-axis, while the normal-incident laser propagates in x-direction. The three numbers are the propagation of beam and laser in order of time precedences: beam at the left top of the laser pulse, beam at center, and beam at the right bottom. It is implied that the beam always moves inside a diagonal area of the rectangular pulse shape. Consequently, a tilted pulse is equivalent to a full rectangular pulse as seen by the beam. Therefore, the interaction length can extend to the entire transverse width of the laser pulse, which is on the order of several centimeters, long enough to realize the FEL exponential growth process, leading to a significantly enhanced coherent radiation.

It should be emphasized that the synchronization between the laser and beam is realized by using pulse front tilt, whose technology has been used in precise synchronization of fast electron diffraction [17, 20]. In our methods, the two lateral lasers could come from the split of a single laser after a single grating structure to avoid the timing jitter between lasers. Moreover, sub-100 attoseconds timing jitter between multiple optical pulse trains have been stably generated from mode-locked lasers [21, 22]. The synchronization between the remote optical pulse trains and microwave signal has achieved the rms timing jitter within 1 femtosecond [23], beneficial for synchronization between laser with beam [24]. Moreover, if the laser power is sufficient high, a single laser as a lateral traveling wave could avoid the time jitter and realize a more uniform K distribution, while the basic scheme of the synchronous interaction of beam and laser keeps the same with the standing wave case.

The necessary pulse front tilt γ is determined by the incidence angle α between the laser and highly relativistic beam [17]: $\gamma = \pi/2 - \arctan[\cot(\alpha/2)]$. For a normal incidence $\alpha = \pi/2$, tilt angle is $\gamma = \pi/4$, which can be created by an angular dispersion $d\varepsilon/d\lambda$ from a diffractive grating satisfying [18, 19], $\gamma = \arctan[\lambda_0(d\varepsilon/d\lambda)]$. The angular dispersion $d\varepsilon/d\lambda$ is calculated from the groove spacing d and the incidence angle θ between the laser and the grating [17], $\varepsilon(\lambda) = \arcsin[\lambda/d - \sin(\theta)]$. For $\lambda_0 = 10$ μm and $\theta = 45^o$, a grating of 97 grooves per millimeter is demanded.

The dimensionless strength parameter $K = eB_{\rm eff}\lambda_u/(2\pi mc)$, where the equivalent magnetic field $B_{\rm eff} = 2E_{y,m}/c$; or we can write $K = 2eE_{y,m}\lambda/(2\pi mc^2)$ for the undulator period $\lambda_u = \lambda$. The peak field at the grating elements is limited by its breakdown thresholds, which is about 2 J/cm^2 for an ultra-short laser pulse with $\tau < 1$ ps [25] for the commercial high power gratings. The cylindrical lenses located between the grating structure and interaction area further enhance the peak field by focusing the transverse size, while keeping the synchronously delayed time of the laser with the electrons. Thus, K reaches 1 to 2 for laser with wavelength 10 μm at the vacuum interaction area.

The influence of laser intensity on the resonant wavelength is important, by aspheric lens pairs, the transverse intensity profile of laser can be transformed from a Gaussian beam to a flat-top beam, whose field $E_{y,m}$ is illustrated in Fig. 2 (b), and the rms flatness of power intensity for the flat-top has been improved to 0.23 % [26]. Because of the relation $\Delta P/P = 2\Delta E/E$, the rms flatness of electric field has reached 0.12 %.

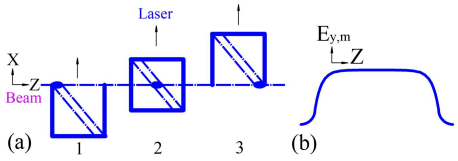

FIG. 2: (a) Equivalence of the tilted pulse and a full rectangular pulse; (b) side view of the flat-top laser.

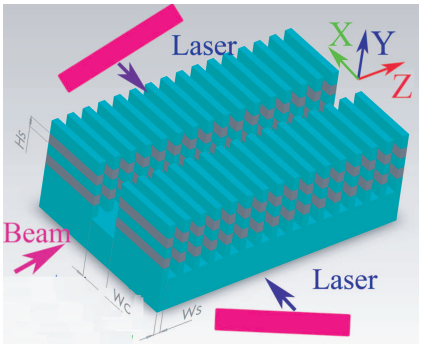

FIG. 3: The 3D view of the periodic microstructure for the interaction of electrons and bi-laterally fed lasers with pulse front tilt; the vacuum channel width W_c, and the height H_s and width W_s for the silicon waveguide.

The second method for enhancing the central electro-

magnetic field is to design a microstructure, including a central electron-beam vacuum channel and periodic-quadrupole dielectric waveguides, which have periodically varying index of refraction (silicon and vacuum) along the channel. Full-wave 3-D electromagnetic simulation HFSS software [27] is used to study the microstructure. Two optical plane waves at normal incidence to the beam channel with the equal amplitude, same polarization and identical phase are oppositely and laterally coupled into this optical structure, as illustrated in Fig. 3. The polarized electric fields E_y are perpendicular to the central Z axis of the channel. When the two incident waves arrive at the central vertical YZ plane, the electric fields with the same polarization and identical phase form a resonant standing wave, leading to a significant enhanced amplitude, and the central YZ plane is equivalent to a magnetic boundary by symmetry. In order to further strengthen the central field, a quasi-quadrupole structure shown in Fig. 3 is designed, where the bi-lateral lasers are guided and propagated in the bi-lateral upper and lower waveguides, which are separated by a substrate layer. The incident phases in the ipsilateral upper and lower waveguides are the same so that the y-directional polarized electric field adds, and there is the strongest field at the center of the quadrupole aperture, as illustrated in Fig. 4. By symmetry, the horizontal XZ plane is equivalent to an electric boundary. The crystalline silicon with high index of refraction is selected as the material of the dielectric waveguides, SiO_2 or sapphire with lower refractive index is applied as the substrates.

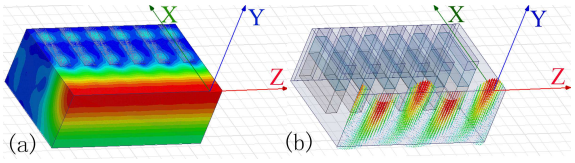

FIG. 4: (a) The complex magnitude field in the quarter of the quadrupole structure. (b) Snapshot of the electric field vector on the central vertical plane. Electron beams fly towards +Z direction.

By adjusting the periodic incident phases of the optical waves, a nonzero phase difference $\Delta\phi$ between the adjacent waveguides along Z-direction is generated, which results in a traveling wave along the central channel, a -11 dB reflection loss of incident wave, and its snapshot electric field are illustrated as Fig. 4. When the flying direction is opposite to the energy flow, relativistic electrons meet a backward wave, and undergo the sum of electric and magnetic forces. For a channel width $W_c \sim 1.3\lambda$, the optimized center field distribution is shown as the red curve in Fig. 5, which implies that the field is distinctly strengthened with the ratio $E_{y,m}/E_m \sim 1.7$, corresponding to a total force $(E_{y,m} + cB_{x,m}) \sim 3.4E_m$.

In Ref. [28], an optical Bragg waveguide with an inner diameter 0.2λ and a corresponding $E_{y,m}/E_m < 0.5$ was proposed to enhance the X-ray brightness by two

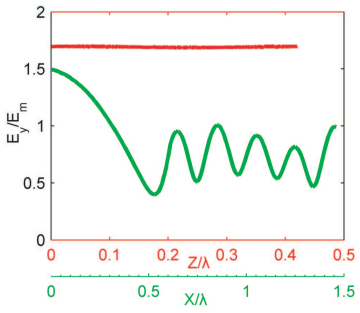

FIG. 5: The normalized complex magnitude of electric field E_y/E_m along the center line of the Si waveguide in X direction (Green curves) and along the central line of quadrupole channel in Z direction (Red curves) for $W_c = 1.3\lambda$, $H_s = 0.3\lambda$, $W_s = 0.19\lambda$, $L_0 = 0.42\lambda$, $\Delta\phi = 0.72\pi$, E_m is the peak field in the waveguide.

orders since the laser is guided and focused inside the channel. As a comparison, the channel width 1.3λ and $E_{y,m}/E_m \sim 1.7$ for our structure are much better than those in the Bragg waveguide. With regard to fabrication, a 3-D micro-structure with a 3 cm long and detailed size ~ 1 μm has been demonstrated since 1996 [29].

The rms opening angle σ of the forward cone of X-ray radiation for undulator periods $N = 5000$, rms $K = 1$, and $\gamma = 100$ is $\sigma = 1.5 \times 10^{-4}$ rad [30], the transverse width of the radiation cone $\sigma L \sim 4.5$ μm for $L = 3$ cm, smaller than the half channel width. Thus, the dielectric channel walls do not influence the main X-ray radiation.

The beam quality has important influence on FEL [31]. Laser-driven plasma accelerator could deliver high-quality electron beams [32, 33]. Recently, the high-brilliant beam was generated with peak current 10 kA, normalized emittance of $\varepsilon_n = 0.3-0.4$ πmm-mrad, beam energy 125 MeV, charge 10 pC, and beam size 1 μm [34]. By X-ray spectroscopy measurement, an ultra low $\varepsilon_n = 0.1$ πmm-mrad was demonstrated with beam energy 450 MeV, and bunch radius 0.1 μm [35]. Since the beam size 1 μm or even 0.1 μm is much smaller than the CO_2 laser wavelength and laser transverse dimension, beam mainly sees a uniform field; besides, the beam size could be much smaller than the channel width 13 μm.

We model the above described process of method one as an effective optical undulator. The electron bunch has centroid energy 60 MeV, $\sigma_\gamma = 0.06$, normalized emittance of $\varepsilon_{n,x(,y)} = 0.2$ πmm-mrad in both x- and y-plane, and peak current $I_{pk} = 3$ kA. There is no focusing channel. The initial bunch transverse size is $\sigma_{x(,y)} = 10$ μm. For this setup, the optical undulator period is $\lambda_u = 10$ μm, assuming a CO_2 laser, and the effective undulator rms parameter $K = 1.5$. With this set of parameters, the FEL Pierce parameter is about $\rho = 3.0 \times 10^{-4}$ [8, 12], hence the saturation power at the end of exponential growth is about 140 MW [36]. We double check this analytical calculation against GENESIS simulation [37].The GENESIS code has been demonstrated to be correct in

optical undulator, since the analytical theory [15] and the code built for optical undulator [14, 38] were consistent with the GENESIS simulation. The simulated FEL power is shown as the red solid curve in Fig. 6; the analytical power with gain length $L_G = 0.7$ mm [8, 12] is the dashed red curve. With a total charge of 50 pC, there are about 1.4×10^{10} photons/pulse. By using MHz repetition-rate lasers, this source has the capacity of generating high-repetitive X-ray photon of 10^{16} to 10^{17}/s.

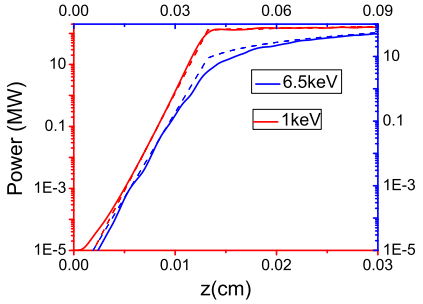

FIG. 6: Genesis simulation (solid red) of a 1 keV FEL together with analytical results (dashed red) and that (solid blue) of a 6.5 keV FEL together with analytical results (dashed blue).

To compare the hard X-ray of 6.5 keV as reported in Ref. [13], the centroid energy of electron bunch is 117 MeV, with the same other parameters and conditions as those for the above 1 keV FEL case. The FEL Pierce parameter is about $\rho = 2.0 \times 10^{-4}$ [8, 12], hence the saturation power is about 50 MW [36]. Similarly, the GENESIS simulated FEL power and analytical power with $L_G = 2.5$ mm are shown as the solid and dashed blue curves in Fig. 6, where a linear power growth is seen after the exponential growth ceases. With a total charge of 60 pC, there are about 1.0×10^9 photons with a 10 to 20 fs duration, in contrast to 2×10^7 photons in a 3.5 ps pulse reported in Ref. [13].

Besides, if the quality of laser and beam does not support a high-gain FEL, for the spontaneous undulator radiation, the total photon flux in the forward cone is proportional to the square of the undulator periods N, and the total flux in the opening angle is proportional to N [30]. Thus, the proposed lateral tilted lasers could significantly improve the total X-ray flux by extending the number of undulator periods in several orders.

To restate, by invoking two pulse front tilted lateral lasers, high-gain exponential growth is made possible to generate FEL-type X-ray source via Thompson Scattering. The critical improvement is lengthening the electron-laser synchronic interaction time by several orders; cylinder lenses or periodic micro-structure are adopted to enhance the central electric field, realizing the high photon number 10^9 to 10^{10} with femtoseconds duration, and the brightness enhanced by 4 to 5 orders.

The work of CC and JW was supported by DOE under contract DE-AC02-76SF00515.

[1] P. Emma *et al.*, Nature Photonics **4**, 641 (2010).
[2] V. Malka *et al.*, Science **298**, 1596 (2002).
[3] J. Faure *et al.*, Nature **431**, 541 (2004).
[4] X. Davoine *et al.*, Phys. Rev. Lett. **102**, 065001 (2009).
[5] M. Fuchs *et al.*, Nature Phys. **5**, 826 (2009).
[6] R. Schoenlein *et al.*, Science **274**, 236 (1996).
[7] A. Gover and P. Sprangle, IEEE J. Quant. Electron. **17**, 1196 (1981).
[8] C. Pellegrini, Rev. Accel. Sci. Tech. **3**, 185 (2010).
[9] D. Attwood, *Soft X-rays and Extreme Ultraviolet Radiation: Principles and Applications*, Cambridge University Press, Cambridge, 1999.
[10] A. Thompson *et al.*, Phys. Rev. Lett. **108**, 145002 (2012).
[11] C. Sun *et al.*, Phys. Rev. ST Accel. Beams **12**, 062801 (2009)
[12] C. Pellegrini and S. Reiche, IEEE J Sel Top Quant Electron **10**, 1393 (2004).
[13] M. Babzien *et al.*, Phys. Rev. Lett. **96**, 054802 (2006).
[14] V. Petrillo *et al.*, Phys. Rev. ST Accel. Beams **11**, 070703 (2008).
[15] P. Sprangle *et al.*, Phys. Rev. ST Accel. Beams **12**, 050702 (2009).
[16] K. Nakajima, Nature Phys. **4**, 92 (2008).
[17] P. Baum and A. Zewail, Proc. Natl. Acad. Sci. **103**, 16105 (2006).
[18] J. Hebling, Opt. Quantum Elec. **28**, 1759 (1996).
[19] J. Fülöp and J. Hebling, *Applications of Tilted-Pulse-Front Excitation*, in "Recent Optical and Photonic Technologies" 2010, INTECH, Croatia.
[20] P. Baum *et al.*, Science **318**, 788 (2007).
[21] T. Kim *et al.*, Opt. Lett. **36**, 4443 (2011)
[22] A. Benedick *et al.*, CLEO: S and I 2011: CFK4, MD, USA.
[23] K. Jung *et al.*, Opt. Lett. **37**, 2958 (2012).
[24] J. Byrd *et al.*, Nucl. Instr. Meth. A **623**, 910 (2010).
[25] D. Du *et al.*, Appl. Phys. Lett. **64**, 3071(1994).
[26] J. Liang *et al.*, Appl. Opt. **49**, 1323 (2010).
[27] ANYS SHFSS software, ANSYS, Inc., USA.
[28] V. Karagodsky *et al.*, Phys. Rev. lett. **104**, 024801 (2010).
[29] X. Zhao *et al.*, Adv. Mater. **8**, 837 (1996).
[30] H. Wiedemann, Particle Accelerator Physcis, Springer, 2007.
[31] B. Jia *et al.*, Phys. Rev. ST Accel. Beams **13**, 060701 (2010)
[32] O. Lundh *et al.*, Nature Phys. **7**, 219 (2011).
[33] S. Fritzler *et al.*, Phys. Rev. Lett. **92**, 165006 (2004).
[34] E. Brunetti *et al.*, Phys. Rev. lett. **105**, 215007 (2010).
[35] G. Plateau, *et al.* Phys. Rev. lett. **109**, 064802 (2012).
[36] M. Xie, Proc. 1995 PAC, p.183, Dallas, Texas, 1995.
[37] S. Reiche, Nucl. Instr. Meth. A **429**, 243 (1999).
[38] C. Maroli *et al.*, Proc. 29^{th} FEL, 244, Russia, 2007.